Reprinted from

JOURNAL OF THE PHYSICAL SOCIETY OF JAPAN

JOURNAL OF THE PHYSICAL SOCIETY OF JAPAN

http://jpsj.jpap.jp/

FULL PAPER

Transmission of Acoustic Waves from a Solid Cylinder into a Liquid and Equivalent Acoustic Impedances

Hatsuyoshi Kato and Hatsuhiro Kato

J. Phys. Soc. Jpn. **83**, 044602 (2014)

Journal of the Physical Society of Japan **83**, 044602 (2014)
http://dx.doi.org/10.7566/JPSJ.83.044602

Transmission of Acoustic Waves from a Solid Cylinder into a Liquid and Equivalent Acoustic Impedances

Hatsuyoshi Kato[1]* and Hatsuhiro Kato[2]

[1]*Tomakomai National College of Technology, Tomakomai, Hokkaido 059-1275, Japan*
[2]*University of Yamanashi, Kofu 400-8511, Japan*

(Received August 29, 2013; accepted January 27, 2014; published online March 12, 2014)

We discuss the feasibility of the one-dimensional theory by which the transmission of acoustic waves from a solid cylinder into a liquid is analyzed with the acoustic impedance. For this purpose, experiments were performed on a cylinder made of Cu with a size of 1.98 $mm^{\phi} \times 51.96\,mm^{t}$. The frequency of acoustic waves was varied from 0.80 to 1.3 MHz. The characteristics of the Pochhammer mode in the solid cylinder are clarified by certain equivalent acoustic impedances. At low frequencies from 0.80 to 1.0 MHz, several definitions of the equivalent acoustic impedances work effectively. At intermediate frequencies near 1.1 MHz, the equivalent impedances available are those defined near the lateral surface of the cylinder. At high frequencies from 1.15 to 1.3 MHz, the experimental transmission rate of acoustic waves decreases considerably, and the adequate impedance is obtained using the energy flux and the axial component of the velocity field in the cylinder.

1. Introduction

The transmission property of acoustic waves from the cylinders into water is one of the important applications.[1)] We have reported experiments on longitudinal waves transmitted into water from thin cylinders or disks made of Cu with a size of $30.0\,mm^{\phi} \times 10.0\,mm^{t}$, of Ag with a size of $30.0\,mm^{\phi} \times 8.0\,mm^{t}$, and of periodically layered Cu and Ag with a size of $30.0\,mm^{\phi} \times 0.5\,mm^{t}$.[2,3)] Furthermore, the transmission rate has been analyzed with the acoustic impedance using a one-dimensional theory. However, the specimens used did not have a large length in the axial direction. In this paper, we discuss the limitation of the one-dimensional acoustic impedance theory in a long solid cylinder.

Historically, the theory of acoustic waves governed by the Pochhammer frequency equation in infinitely long cylinders was first published in 1876.[4,5)] However, owing to its complexity, detailed discussions appeared only from the 1940s.[6,7)] In those initial works, Pochhammer modes were treated with other modes like flexural modes and torsional modes.[6)] As the frequency is increased indefinitely, one branch of Pochhammer modes approaches the Rayleigh surface mode, which has a velocity less than the velocity of the transverse mode in bulk media, and the phase velocities of the other branches approach the transverse mode velocity.[7)] The detailed dispersion relations of Pochhammer mode were discussed by Onoe et al. including real, pure imaginary, and complex branches.[8)] In experiments on traveling acoustic wave pulses, it was shown that wave forms of pulses deform widely in space at a certain frequency.[9)] This deformation originates from the coupling of the Pochhammer mode with one of the flexural modes due to the imperfectness of the lateral surface. In the dispersion branches of Pochhammer modes, the phase velocity and the group velocity have opposite directions.[10)] This is called backward-wave transmission and, in this case, the directions of energy flux are opposite those of the phase velocities.

The features of traveling acoustic waves in the cylinders resemble those of wave guides with a rectangular cross section or plates, and they are often discussed simultaneously.[11)] In this case, extensional motions in isotropic media were treated by two-dimensional approximation, and dispersion relations were compared with those by three-dimensional approximation,[12)] and it was shown that the exact solutions for bars with an infinite length are composite of dilation and equivoluminal waves.[13)] Furthermore, waves in anisotropic media were discussed by one-dimensional approximation, in which waves in a rectangular cross section were expanded with Legendre polynomials, and those in a circular cross section with Jacobi polynomials.[14)]

To avoid the intricate boundary conditions in acoustics for semi-infinite media, it is effective to employ analogies of the electric transmission line theory with characteristic impedances.[15)] By this method, it is possible to consider acoustic waves in liquids, P-, SV-, and SH-waves in bulk solids, Rayleigh surface waves, leaky Rayleigh waves, Lamb waves, and Love waves. The boundary conditions are treated as equivalent circuits connected to transmission lines. The correspondences for the characteristic impedances in electricity are the acoustic impedances, which resemble the stiffnesses in elastic theories.

Experimentally, elastic constants were obtained to determine the velocities of pulses.[16,17)] In those works, compliances extended to complex values were measured, and their reciprocals were related to acoustic impedances.

For examples of applications and interests, elastic plates on rigid solids are applied as acoustic wave guides,[18,19)] and, in recent years, at frequencies of up to several GHz, the vibrational properties have been studied in nanostructures in which gold plates or copper wires are periodically arranged.[20,21)] Furthermore, in cylinders that have a volume of 0.3 μm^3 and heights of 4–5 μm, a whispering gallery mode was observed,[22)] and in thin cylinders and/or disks acoustic vibrational motions were analyzed theoretically.[23)] Furthermore, poly(methyl methacrylate) micro/nanobeams with a length of 0.1 μm, a width of 0.05 μm, and a thickness up to as low as 47 nm were fabricated, and Young's modulus was trimmed experimentally.[24)]

In this paper, we concentrate on the transmission property of Pochhammer mode from Cu cylinder into water. In Sect. 2, experimental devices and their configuration are explained briefly. In Sect. 3, experimental results are

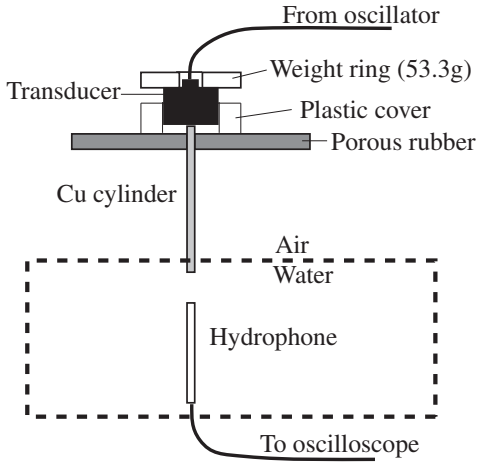

Fig. 1. Configuration of the experiment. The transducer is driven by the oscillator and the acoustic waves are sent to the Cu cylinder. Waves transmitted from the cylinder to the distilled water are detected by the hydrophone.

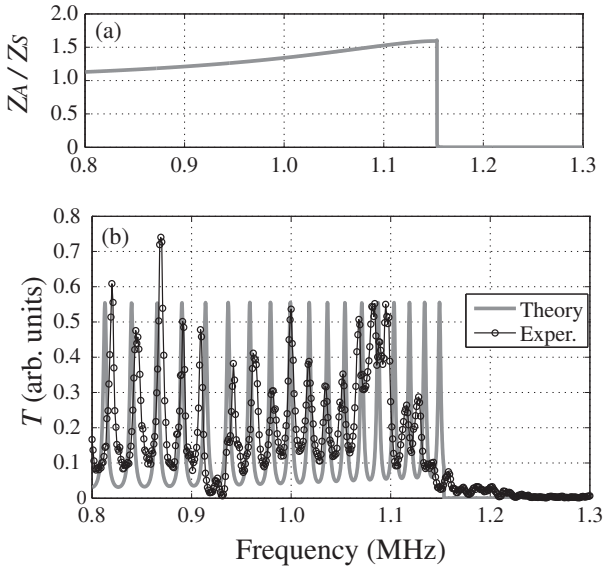

Fig. 2. (a) Ratio of the Cu impedance Z_A to the mean equivalent impedance (MEI) Z_S calculated theoretically and (b) transmission rates obtained by experiments and theory with MEI in one-dimensional approximation.

compared with the theory with a one-dimensional impedance. In Sect. 4, we examine another definition of acoustic impedances and clarify the characteristics of the Pochhammer mode. In Sect. 5, we summarize the results.

2. Experimental Procedure

The specimen for the experiment is a solid cylinder made of Cu, with a diameter of 1.98 mm and a length of 51.96 mm. It is supported by a porous rubber layer with a thickness of 5 mm, as is shown in Fig. 1; its end is raised by 3 mm. The upper end of the cylinder is in contact with the ultrasonic transducer using silicone grease as couplant. The transducer is in a plastic cover to make sure that its contact plane is parallel to the specimen's end on the porous rubber layer. Furthermore, the transducer is weighted down by a ring with a mass of 53.3 g for steady contact with the end of the cylinder. The transducer itself weighs 21.0 g.

The transducer is connected to the oscillator and driven by an RF voltage of 7.07 V_{pp}, and its exerted frequencies are from 0.80 to 1.3 MHz in steps of 1 kHz. The lower end of the cylinder (3 mm) is immersed in distilled water (0.06×10^{-4} S/m), and the sensor of hydrophone is set 7 mm below the end of the cylinder in water. Pressure signals in water are received by the hydrophone and sent to the amplifier (oscilloscope). They are then processed by FFT to extract the strength of the transmitted acoustic waves with the same frequencies as those of the transducer exertion. The time window is 1.00 ms for the FFT. The distilled water has a volume of 7.7 L and is foamless.

To protect the transducer in the experiments, at each frequency, the transducer was intermittently excited by the oscillator with a 3.0-s mark after a 1.0-s space. One millisecond later from the beginning of the mark, signals from the hydrophone were started to be obtained for the analysis by FFT. Therefore, in the Cu cylinder, the stationary waves were grown up as in the case of CW excitations. The effect of multiple reflections between the hydrophone and the Cu cylinder and/or water surface was neglected, because, before the experiments, the numerical calculations by FEM showed no remarkable evidence that multiple reflections interfered with the measurements of acoustic waves that reached the hydrophone directly from the Cu cylinder. In the experiments, we may assume that the acoustic waves were scattered by the hydrophone sensor with a diameter of 1.4 mm at the tapered tip and by the support of hydrophone placed underwater within a vertical depth 15 cm, and they then spread and weakened in the water bath with a horizontal area of 30×17 cm^2.

The experiments were performed at room temperature at atmospheric pressure (22.5 °C, 1015 hPa), and the temperature of distilled water was 20.5 °C.

3. Experimental Results and Theory

Transmission rates were obtained by experiments on acoustic waves generated by the transducer and measured through the cylinder as the Pochhammer mode and penetrated into the distilled water as pressure waves. They are shown in Fig. 2(b). The experiments were repeated six times and the measured transmission rates were averaged. At frequencies from 0.80 to 1.0 MHz, the peaks of the transmission rates appear with wider frequency intervals. At frequencies near 1.1 MHz, the peak intervals become narrower, and the dips become shallower. Furthermore, at frequencies from 1.15 to 1.3 MHz, the transmission rates become almost null, and there are no pressure waves in water. Also, at a frequency of 0.931 MHz, there are no waves in water. This is due to the coupling of the Pochhammer mode with the flexural mode.[9)]

In a one-dimensional transmission model of acoustic waves that pass through the semi-infinite plate A with a thickness d from material O (transducer) to material W (water), the transmission rate T is expressed as

$$T = \frac{4Z_O/Z_W}{(1 + Z_O/Z_W)^2 \cos^2 kd + (Z_O/Z_A + Z_A/Z_W)^2 \sin^2 kd}, \quad (1)$$

where the phase factor of the acoustic waves is assumed as $e^{-ikz+i\omega t}$, which is also the same as the factor of the Pochhammer mode. Further, z and k are, respectively, the

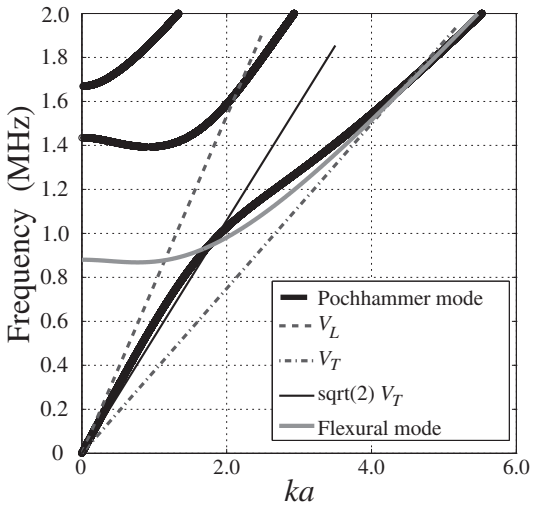

Fig. 3. Dispersion of Pochhammer modes and the flexural mode with which the Pochhammer mode couples. Dispersions for the longitudinal and transverse modes in bulk Cu are shown; furthermore, the line corresponding to the phase velocity $\sqrt{2}V_T$ is also depicted as a guide for the eyes.

coordinate perpendicular to the plate and wave number. The acoustic impedances are Z_O for the transducer, Z_A for the plate, and Z_W for water.

When we apply the one-dimensional model to the cylinder, the waves transmittable into water are dilatation waves [see Eq. (A·11) in Appendix]. However, equivoluminal waves [see Eq. (A·12) in Appendix] must also be considered, because the free surface conditions of the lateral surface of the cylinder cannot be satisfied without equivoluminal waves.[9]

To seek the one-dimensional equivalent acoustic impedance that can be substituted for the acoustic impedance Z_A of the semi-infinite plate in Eq. (1), we discuss the energy flows in an infinite cylinder. The axial coordinate z is set along the cylinder, and the radial coordinate r and the angular coordinate ϕ are set in a circular cross section. The angular frequency is denoted as ω. The lateral surface is assumed to be a free surface, and the vibrations in the ϕ directions are omitted. In this case, the acoustic waves satisfy the Pochhammer frequency equation[5] in infinitely long cylinders. The lower branches of the dispersion relations are shown in Fig. 3. In the case of our experiments, the first branch of the Pochhammer mode is concerned. In Fig. 3, a branch of the flexural mode is also depicted, and it crosses the first branch of the Pochhammer mode at 0.975 and 1.783 MHz theoretically.

The energy does not flow in the r- or ϕ-direction, and only the nonzero component of the Poyinting vector is in the z-direction denoted as $P_z(r)$. The total energy flux is obtained by integrating it as

$$J_z = \int_0^a 2\pi r P_z(r)\, dr, \tag{2}$$

where a is the radius of the circular cross section. The z-component $v_z(r)$ and the r-component $v_r(r)$ of the velocity field contribute the energy flows in the cylinder. The main contribution to the transmission into water is the energy flow by $v_z(r)$. When we assume that the z-component of the velocity field is uniform in the circular cross section and put it as $\dot{u}$, then the total energy flux can be approximately expressed as

Table I. The parameters used in the theoretical calculations are density ρ, Young's modulus E, Poisson ratio ν, transverse mode velocity V_T, longitudinal mode velocity V_L, and acoustic impedance $Z = \rho V_L$ for longitudinal mode in bulk media. Lamé constants of Cu become $\lambda = 10.558 \times 10^{10}$ Pa and $\mu = 4.8325 \times 10^{10}$ Pa.

	ρ (g cm^{-3})	E (Pa)	ν —	V_T (km s^{-1})	V_L (km s^{-1})	$Z = \rho V_L$ (kg m^{-2} s^{-1})
Cu	8.93	12.98×10^{10}	0.343	2.3263	4.7587	2.495×10^6
H_2O	0.999	—	—	—	1.483	1.482×10^6

$$\frac{J_z}{\pi a^2} \simeq \frac{2}{a^2}\int_0^a \frac{rP_z(r)}{\frac{1}{2}|v_z(r)|^2}\frac{1}{2}|\dot{u}|^2\, dr = \frac{1}{2}Z_S|\dot{u}|^2. \tag{3}$$

In this approximation, we define $Z(r)$ and Z_S as

$$Z(r) = \frac{P_z(r)}{\frac{1}{2}|v_z(r)|^2}, \tag{4}$$

$$Z_S = \frac{2}{a^2}\int_0^a rZ(r)\, dr \equiv \langle Z\rangle. \tag{5}$$

We call the above quantities as the local equivalent impedance (LEI) and mean equivalent impedance (MEI), respectively. The notation $\langle\cdots\rangle$ expresses the mean across the circular cross section. The explicit form of Eq. (4) is explained in Appendix B.2. In the above expressions, we emphasize the dependences on the radial coordinate r, however, they also depend on the frequency. The ratio of the acoustic impedance Z_A of bulk Cu to Z_S in Eq. (5) is shown in Fig. 2(a) against the frequency. The theoretical transmission rates are calculated using Z_S instead of Z_A in Eq. (1) and are shown in Fig. 2(b). The thickness d is set as the length of the Cu cylinder. We have estimated $Z_O = 5Z_W$ from the swinging widths vs frequencies of the experimental transmission rates. In the frequency range from 0.80 to 1.0 MHz, Z_S has finite values and the transmission rates calculated theoretically have certain agreement with those of the experiments. In the vicinity of 1.1 MHz some discrepancies have occurred, which is discussed in the next section. In the range from 1.15 to 1.3 MHz, the acoustic waves in the cylinder are not transmitted to water as is shown in Fig. 2(b) both theoretically and experimentally. The theoretical calculation shows $Z_S \to \infty$ ($Z_A/Z_S \to 0$), and the transmission is suppressed. In such a frequency range, $P_z(r) \neq 0$ in spite of $v_z(r) = 0$, which means the energy flows by the r-component of the velocity field. Therefore, on the lower end of the Cu cylinder immersed in water, the shear components $v_r(r)$ are higher than the pressure components $v_z(r)$, and the transmission rate vanishes.

The parameters used in the theoretical calculation are summarized in Table I.

4. Discussion

At frequencies from 1.0 to 1.1 MHz, as shown in Fig. 2(b) in the previous section, the theoretical transmission rates have discrepancies from those of the experiments whose troughs have higher values than the theoretical values. When we substitute $Z(a)$ for Z_A in the transmission formula Eq. (1), the calculated transmission rates become as is shown in

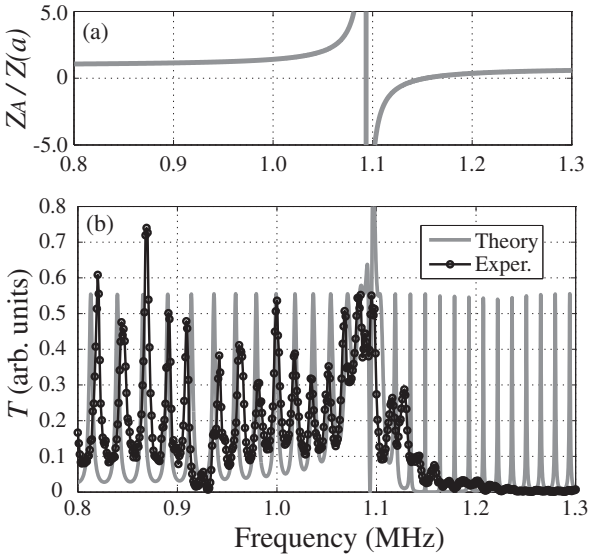

Fig. 4. (a) The ratio of Z_A to $Z(a)$ that is the local equivalent impedance (LEI) at $r = a$ is shown. (b) The transmission rates theoretically calculated with $Z(a)$ and the experimental results are shown.

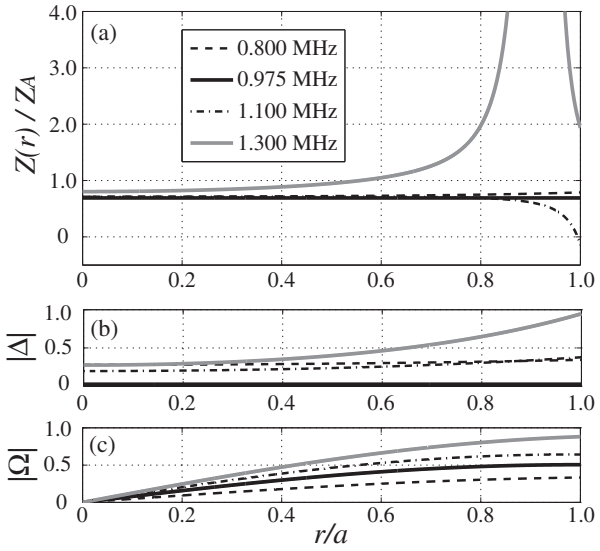

Fig. 5. (a) A plot of LEIs at some frequencies vs radius of the cross section is depicted. Furthermore, (b) the absolute value of the dilatation Δ in arbitrary units and (c) the absolute value of the rotation Ω in arbitrary units are shown. All values are of the cylinder with an infinite length.

Fig. 4(b), where $Z(a)$ is the LEI defined by Eq. (4) at $r = a$. The ratio of Z_A to $Z(a)$ is also shown in Fig. 4(a). With the substitution, the transmission rates show agreement in a wide frequency range from 0.80 to 1.1 MHz. This implies that the LEIs are almost the same as those of the MEI at any point in the circular cross section of the Cu cylinder.

However, in the upper range of over 1.14 MHz, $Z(a)$ cannot explain the suppression of the transmission rate.

The theoretical LEI $Z(r)$ is plotted against r at several frequencies in Fig. 5(a). From 0.80 to 1.0 MHz, the LEIs are almost the same. Especially, at 0.975 MHz, the values of $Z(r)$ are exactly the same as $Z(a)$; also, $Z(r)$ does not depend on r. $Z(r) = \rho\omega/k$, where ρ is the density of Cu and ω/k is the phase velocity $\sqrt{2}V_T$. This frequency corresponds to 0.931 MHz experimentally, and the Pochhammer mode couples with the flexural mode.[9)]

At frequencies near 1.1 MHz, the LEIs are lower near the lateral surface, $r/a = 1$, than near the center. Therefore, the energy flows near the lateral surface. This is also clear when we see the dilatation and rotation shown in Figs. 5(b) and 5(c), respectively, where both values are large near the lateral side. This is the reason why the transmission rates can be explained by the LEI $Z(a)$ in the wide frequency range. Furthermore, the first branch of the Pohhammer mode and the branch of the flexural mode separate from each other, as shown in Fig. 3 from 0.975 to 1.783 MHz. Therefore, the effects of the flexural mode is weakened at these frequencies.

At frequencies higher than 1.15 MHz, as shown in Fig. 5(a), the LEI $Z(r)$ has infinitely large values at a certain place on the cross section. As a result, the transmission rate becomes lower. Because the Pochhammer mode also couples with the flexural mode at a frequency of 1.783 MHz, the transmission of the acoustic waves into water should be suppressed experimentally at these frequencies.

When we equate $|\dot{u}|^2$ in Eq. (3) with $\langle|v_z(r)|^2\rangle$, another MEI can be obtained (see Appendix B.1) as follows:

$$\bar{Z} = \frac{J_z/\pi a^2}{\frac{1}{2}\langle|v_z|^2\rangle} = \frac{\langle P_z\rangle}{\frac{1}{2}\langle|v_z|^2\rangle}. \tag{6}$$

When we substitute $\bar{Z}$ for Z_A in Eq. (1), the theoretical transmission rates show agreement with the experimental values at frequencies lower than 1.0 MHz. We also obtained the same results using other expressions of equivalent impedances explained in Appendix B. At lower frequencies, these definitions are almost equal to the well-known expression $Z_A \simeq \rho\omega/k$ in the bulk, as is shown in Fig. 5(a).[2,3)]

A theoretical analysis of acoustic waves in a *finite* cylinder has already been published[23)] in which some modes have been discussed to become Pochhammer modes asymptotically. However, it is more complicated than the theory of one-dimensional acoustic impedances derived from the Pochhammer mode of the *infinite* cylinder discussed in the present paper. Furthermore, for an infinitely long elastic waveguide with various cross sections including a circular cross section, the propagating and evanescent waves have also been discussed numerically.[25)] In the work, the transmission of the waves into a liquid has not yet been treated. It could be expanded to discuss transmission into a liquid accurately. However, even though the accuracy is limited, the method using the MEI, LEI and wave transmission into a liquid is rather concise and intuitive for the analysis of the Pochhammer mode, as discussed in the present paper.

5. Conclusions

By experiments on acoustic waves in a Cu cylinder with a size of 1.98 mm$^{\phi}$ × 51.96 mm^{t} at frequencies from 0.80 to 1.3 MHz, the characteristics of the Pochhammer mode are clarified, e.g., the mode does not penetrates water at frequencies higher than 1.15 MHz.

In the frequency range lower than the frequency at which the Pochhammer mode couples with the flexural mode, several definitions of equivalent impedances are effective. For

the application of acoustic wave transmission from the cylinder into water, it is recommendable to use frequencies lower than the frequency at which the coupling occurs. In the case of our specimen, the frequencies are lower than 0.931 MHz. At these lower frequencies, we can also use the normal acoustic impedance as is defined for thin disks as $Z_A \simeq \rho\omega/k$.

At intermediate frequencies near 1.1 MHz, the effective impedance that can explain the frequency dependence of the transmission rate is defined by the LEI on the lateral surface of the cylinder expressed by Eq. (4) with $r = a$. At such frequencies, the energy transmittable to water flows near the lateral surface, where the LEIs are lower.

In the frequency range higher than 1.15 MHz, the effective impedance can be defined using the energy flux and the axial component of the velocity field, i.e., the MEI defined by Eq. (5). At such frequencies, acoustic wave transmission does not occur, because the axial component of the velocity field vanishes in spite of the existence of an energy flow. This means that the energy is carried by the radial component of the velocity field, and that the shear components for water become higher than the pressure components.

The effective impedances suitable in the target frequency range must be selected, as we have concluded above for the one-dimensional theory of finite cylinders. The method of defining the equivalent acoustic impedance using the energy flux is feasible for application in other acoustic waveguides that do not have circular cross sections.

Acknowledgment

The present study was partly supported by KAKENHI (23560065).

Appendix A: Energy Flux in Cylinders

In isotropic media, the stiffness constants have the relation $c_{11} = 2c_{44} + c_{12}$. Using the Lamé constants, we can also express them as $\lambda = c_{12}$ and $\mu = c_{44}$ respectively; furthermore, Young's modulus and the Poisson ratio are $E = \mu(3\lambda + 2\mu)/(\lambda + 2\mu)$ and $\nu = \lambda/(2\lambda + 2\mu)$, respectively.

In the following discussions, we use the method elucidated by Auld using the particle velocity field $\mathbf{v}$ instead of the displacement $\mathbf{u}$.[26] When media are isotropic and do not have any losses of energy, the time factor is $e^{i\omega t}$ and the velocity field becomes $\mathbf{v} = i\omega\mathbf{u}$. This relation is convenient when we discuss the acoustic impedances. With the stiffness constants and density of the isotropic media, the equation of motion is

$$c_{44}\nabla^2\mathbf{v} + (c_{11} - c_{44})\nabla(\nabla\cdot\mathbf{v}) = \rho\frac{\partial^2\mathbf{v}}{\partial t^2}. \tag{A·1}$$

By introducing the scalar potential Φ and the vector potential $\mathbf{\Psi}$, the velocity field is expressed as

$$\mathbf{v} = \nabla\Phi + \nabla\times\mathbf{\Psi}. \tag{A·2}$$

The equation of motion is then equivalent to the next two equations:

$$\nabla^2\Phi - \frac{1}{V_L^2}\frac{\partial^2\Phi}{\partial t^2} = 0, \tag{A·3}$$

$$\nabla^2\mathbf{\Psi} - \frac{1}{V_T^2}\frac{\partial^2\mathbf{\Psi}}{\partial t^2} = 0, \tag{A·4}$$

where $V_L = \sqrt{c_{11}/\rho}$ and $V_T = \sqrt{c_{44}/\rho}$ are the longitudinal and transverse velocities, respectively, in bulk media.

For the discussion of elastic waves in a cylinder with an infinite length, the velocity field is expressed in the cylindrical coordinates (r, ϕ, z) as $\mathbf{v} = v_r\mathbf{e}_r + v_\phi\mathbf{e}_\phi + v_z\mathbf{e}_z$, where $\mathbf{e}_r$, $\mathbf{e}_r$, and $\mathbf{e}_z$ are the base vectors. We concentrate on azimuthally symmetric modes, i.e., $\partial\mathbf{v}/\partial\phi = 0$; then, the solutions of Eqs. (A·3) and (A·4) are obtained as

$$\Phi = AJ_0(\alpha r)e^{-ikz+i\omega t}, \tag{A·5}$$

$$\mathbf{\Psi} = -\mathbf{e}_\phi BJ_1(\beta r)e^{-ikz+i\omega t}, \tag{A·6}$$

where $\alpha^2 = \omega^2/V_L^2 - k^2$ and $\beta^2 = \omega^2/V_T^2 - k^2$. Using these potentials, the components of the velocity field become

$$v_r = \{-A\alpha J_1(\alpha r) - ikBJ_1(\beta r)\}e^{-ikz+i\omega t}, \tag{A·7}$$

$$v_\phi = 0, \tag{A·8}$$

$$v_z = \{-ikAJ_0(\alpha r) - B\beta J_0(\beta r)\}e^{-ikz+i\omega t}. \tag{A·9}$$

The strain and stress tensors are now calculated with the relation $\mathbf{u} = (1/i\omega)\mathbf{v}$ using the same stiffness constants as those in rectangular coordinates. By using the abbreviated suffixes $\{1,2,3,4,5,6\}$ for $\{rr, \phi\phi, zz, \phi z, zr, r\phi\}$, we can deduce the expression of the stress tensor as

$$\begin{bmatrix} T_1 \\ T_2 \\ T_3 \\ T_4 \\ T_5 \\ T_6 \end{bmatrix} = \begin{bmatrix} c_{11}\dfrac{\partial u_r}{\partial r} + c_{12}\dfrac{u_r}{r} + c_{12}\dfrac{\partial u_z}{\partial z} \\ c_{12}\dfrac{\partial u_r}{\partial r} + c_{11}\dfrac{u_r}{r} + c_{12}\dfrac{\partial u_z}{\partial z} \\ c_{12}\dfrac{\partial u_r}{\partial r} + c_{12}\dfrac{u_r}{r} + c_{11}\dfrac{\partial u_z}{\partial z} \\ 0 \\ c_{44}\left(\dfrac{\partial u_r}{\partial z} + \dfrac{\partial u_z}{\partial r}\right) \\ 0 \end{bmatrix}. \tag{A·10}$$

When we calculate these expressions, the next quantity often appears:

$$\Delta = \frac{\partial v_r}{\partial r} + \frac{v_r}{r} + \frac{\partial v_z}{\partial z} = -A(\alpha^2 + k^2)J_0(\alpha r)e^{-ikz+i\omega t}. \tag{A·11}$$

This is called the dilatation, and the next quantity is called the rotation:

$$\Omega = \frac{1}{2}\left(\frac{\partial v_r}{\partial z} - \frac{v_z}{r}\right) = -\frac{1}{2}B(\beta^2 + k^2)J_1(\beta r)e^{-ikz+i\omega t}. \tag{A·12}$$

The explicit forms of the stress components become

$$i\omega T_1/e^{-ikz+i\omega t} = A\{2c_{44}\alpha^2 J_0''(\alpha r) - c_{12}(\alpha^2 + k^2)J_0(\alpha r)\} + B2c_{44}ik\beta J_0''(\beta r), \tag{A·13}$$

$$i\omega T_2/e^{-ikz+i\omega t} = A\left\{2c_{44}\frac{\alpha}{r}J_0'(\alpha r) - c_{12}(\alpha^2 + k^2)J_0(\alpha r)\right\} + B2c_{44}\frac{ik}{r}J_0'(\beta r), \tag{A·14}$$

$$i\omega T_3/e^{-ikz+i\omega t} = -A\{2c_{44}k^2 + c_{12}(\alpha^2 + k^2)\}J_0(\alpha r) + B2c_{44}ik\beta J_0(\beta r), \tag{A·15}$$

$$i\omega T_4/e^{-ikz+i\omega t} = 0, \tag{A·16}$$

$$i\omega T_5/e^{-ikz+i\omega t} = -Ac_{44}2ik\alpha J_0'(\alpha r) - Bc_{44}(\beta^2 - k^2)J_0'(\beta r), \tag{A·17}$$

$$i\omega T_6/e^{-ikz+i\omega t} = 0. \tag{A·18}$$

When we apply the free-boundary condition on the lateral surface of the cylinder, we have $T_1 = 0$ and $T_5 = 0$ at $r = a$, where a is the radius of the cross section. As a result we have

$$2\frac{\alpha}{a}(\beta^2 + k^2)J_1(\alpha a)J_1(\beta a) - (\beta^2 - k^2)^2 J_0(\alpha a)J_1(\beta a) - 4k^2\alpha\beta J_1(\alpha a)J_0(\beta a) = 0. \quad \text{(A·19)}$$

This is called the Pochhammer frequency equation,[4,5] and its roots give the dispersion relations of acoustic waves. We call these waves the Pohhammer modes in the present paper. Furthermore, we obtain the ratio of the potential amplitudes as

$$\frac{B}{A} = -ik\beta f, \quad \text{(A·20)}$$

where

$$f = \frac{2\alpha J_1(\alpha a)}{(\beta^2 - k^2)\beta J_1(\beta a)}. \quad \text{(A·21)}$$

We discuss the energy flux for the waves of the Pochhammer mode. To obtain the Poynting vector $\mathbf{P}$, we rewrite the stress tensor as

$$\mathbf{T} = \begin{bmatrix} T_1 & T_6 & T_5 \\ T_6 & T_2 & T_4 \\ T_5 & T_4 & T_3 \end{bmatrix} = \begin{bmatrix} T_1 & 0 & T_5 \\ 0 & T_2 & 0 \\ T_5 & 0 & T_3 \end{bmatrix}. \quad \text{(A·22)}$$

The formula that gives the Poynting vector is

$$\mathbf{P} = -\frac{1}{2}\mathrm{Re}[\mathbf{v}^* \cdot \mathbf{T}]. \quad \text{(A·23)}$$

By using the explicit expressions for the components of $\mathbf{v}$ and $\mathbf{T}$, we have $P_r = P_\phi = 0$ and

$$P_z = \frac{|A|^2 k c_{44}}{2\omega}[2\{\alpha J_1(\alpha r)\}^2 + k^2(k^2 - \beta^2)f^2\{\beta J_1(\beta r)\}^2 + (3k^2 - \beta^2)f\alpha J_1(\alpha r)\beta J_1(\beta r) + (k^2 - 2\alpha^2 + \beta^2)\{J_0(\alpha r)\}^2 + 2k^2\beta^4 f^2\{J_0(\beta r)\}^2 + \beta^2(2\alpha^2 - \beta^2 - 3k^2)fJ_0(\alpha r)J_0(\beta r)]. \quad \text{(A·24)}$$

Therefore, the total energy flux $\mathbf{J} = 2\pi\int_0^a r\mathbf{P}\,dr$ has a nonzero component along the axis like

$$J_z = 2\pi\int_0^a rP_z\,dr = \frac{|A|^2 k c_{44}}{2\omega}(k^2 + \beta^2)\pi a^2\left\{Q_\alpha + k^2\beta^2 f^2 Q_\beta + \frac{4f}{a^2}Q_{\alpha\beta}\right\}, \quad \text{(A·25)}$$

where we define

$$Q_\alpha = J_0^2(\alpha a) + J_1^2(\alpha a), \quad \text{(A·26)}$$

$$Q_\beta = J_0^2(\beta a) + J_1^2(\beta a), \quad \text{(A·27)}$$

$$Q_{\alpha\beta} = \alpha a J_1(\alpha a)J_0(\beta a) - \beta a J_0(\alpha a)J_1(\beta a). \quad \text{(A·28)}$$

Appendix B: Equivalent Impedances

We summarize the definitions of equivalent impedances that can explain the experimental transmission rates at frequencies lower than 1.0 MHz. When the condition $\beta = k$ ($\omega/k = \sqrt{2}V_\mathrm{T}$) is satisfied, all impedances explained in the following subsections are the same as $c_{44}2\beta/\omega = \rho\omega/k = \rho\sqrt{2}V_\mathrm{T}$. Furthermore, the dilatations defined by Eq. (A·11) vanish and the rotations defined by Eq. (A·12) have nonzero values. Therefore, the Pochhammer mode has the character of equivoluminal waves or pure shear waves. Furthermore, it couples with the flexural mode under the same conditions.[8,9]

B.1 Mean equivalent impedance 1

When the Pochhammer frequency equation is satisfied, the z-component of the velocity field, Eq. (A·9), becomes

$$v_z(r) = ikA\{-J_0(\alpha r) + \beta^2 f J_0(\beta r)\}e^{-ikz+i\omega t}. \quad \text{(B·1)}$$

The mean square value over the cross section of the cylinder is obtained as

$$\langle|v_z|^2\rangle = \frac{2}{a^2}\int_0^a r|v_z(r)|^2\,dr = k^2|A|^2\left\{Q_\alpha + \beta^4 f^2 Q_\beta - 4f\frac{\beta^2}{(\alpha^2 - \beta^2)a^2}Q_{\alpha\beta}\right\}. \quad \text{(B·2)}$$

With this expression, MEI is defined as

$$\bar{Z} = \frac{J_z/\pi a^2}{\frac{1}{2}\langle|v_z|^2\rangle} = \frac{\langle P_z\rangle}{\frac{1}{2}\langle|v_z|^2\rangle} = \rho\frac{\omega}{k}\frac{Q_\alpha + k^2\beta^2 f^2 Q_\beta + 4f\frac{1}{a^2}Q_{\alpha\beta}}{Q_\alpha + \beta^4 f^2 Q_\beta - 4f\frac{\beta^2}{(\alpha^2 - \beta^2)a^2}Q_{\alpha\beta}}. \quad \text{(B·3)}$$

This is the MEI discussed in the text using Eq. (6). The transmission rates in one-dimensional approximation are calculated by the substitution of $\bar{Z}$ for Z_A in Eq. (1).

B.2 Local equivalent impedance 1

Regarding the cross section at r, LEI is defined as

$$Z(r) = \frac{P_z(r)}{\frac{1}{2}|v_z(r)|^2}, \quad \text{(B·4)}$$

where $P_z(r)$ has been defined in Eq. (A·24) and $v_z(r)$ in Eq. (B·1). When we substitute the mean, $\langle Z\rangle$, of the LEI for Z_A in Eq. (1), we have the transmission rates in one-dimensional approximation. In the text, the LEI at $r = a$, $Z(a)$ has been discussed in Sect. 4. The impedance $\langle Z\rangle$ is different from the $\bar{Z}$ discussed in the previous subsection.

B.3 Mean equivalent impedance 2

When the Pochhammer frequency equation is satisfied, the stress component $T_3 = T_{zz}$ expressed in Eq. (A·15) becomes

$$T_{zz}(r) = \frac{c_{44}}{i\omega}A\{(2\alpha^2 - \beta^2 - k^2)J_0(\alpha r) + 2k^2\beta^2 f J_0(\beta r)\}e^{-ikz+i\omega t}. \quad \text{(B·5)}$$

With the mean of this quantity, $\langle T_{zz}\rangle$, and the mean of Eq. (B·1), $\langle v_z(r)\rangle$, we have another definition of MEI as

$$\bar{Z}_2 = \frac{-\langle T_{zz}\rangle}{\langle v_z\rangle} = -\frac{c_{44}}{k\omega}\frac{4k^2\alpha^2 - (\beta^2 - 2\alpha^2 + k^2)(\beta^2 - k^2)}{\beta^2 - 2\alpha^2 - k^2}. \quad \text{(B·6)}$$

We can also obtain the transmission rates in one-dimensional approximation with the substitution of $\bar{Z}_2$ for Z_A in Eq. (1).

B.4 Local equivalent impedance 2

Another expression of LEI can be defined using Eqs. (B·1) and (B·5) as

$$Z_2(r) = \frac{-T_{zz}(r)}{v_z(r)} = -\frac{c_{44}}{k\omega}\frac{(2\alpha^2-\beta^2-k^2)J_0(\alpha r)+2k^2\beta^2 f J_0(\beta r)}{J_0(\alpha r)-\beta^2 f J_0(\beta r)}. \quad \text{(B·7)}$$

We can also obtain the transmission rates in one-dimensional approximation with the substitution of $\langle Z_2\rangle$ for Z_A in Eq. (1). The impedance $\langle Z_2\rangle$ is different from the $\bar{Z}_2$ discussed in the previous subsection.

*kato@gt.tomakomai-ct.ac.jp

1) G. W. McMahon, J. Acoust. Soc. Am. **36**, 85 (1964).
2) H. Kato and Y. Kojima, Jpn. J. Appl. Phys. **41**, 3202 (2002).
3) H. Kato and Y. Kojima, Jpn. J. Appl. Phys. **42**, 2923 (2003).
4) K. F. Graff, *Wave Motion in Elastic Solids* (Oxford University Press, Oxford, U.K., 1975) p. 470.
5) J. L. Rose, *Ultrasonic Waves in Solid Media* (Cambridge University Press, Cambridge, U.K., 1999) p. 145.
6) D. Bancroft, Phys. Rev. **59**, 588 (1941).
7) G. E. Hudson, Phys. Rev. **63**, 46 (1943).
8) M. Onoe, H. D. McNiven, and R. D. Mindlin, J. Appl. Mech. **29**, 729 (1962).
9) A. H. Meitzler, J. Acoust. Soc. Am. **33**, 435 (1961).
10) A. H. Meitzler, J. Acoust. Soc. Am. **38**, 835 (1965).
11) B. A. Auld, *Acoustic Fields and Waves in Solids* (Krieger, Malabar, FL, 1990) 2nd ed., Vol. 2, Chap. 10, p. 73.
12) R. D. Mindlin and M. A. Medick, J. Appl. Mech. **26**, 561 (1959).
13) R. D. Mindlin and E. A. Fox, J. Appl. Mech. **27**, 152 (1960).
14) M. A. Medick, J. Appl. Mech. **33**, 489 (1966).
15) A. A. Oliner, IEEE Trans. Microwave Theory Tech. **17**, 812 (1969).
16) Y. Sogabe, K. Kishida, and K. Nakagawa, Bull. JSME **25**, 321 (1982).
17) Y. Sogabe and M. Tsuzuki, Bull. JSME **29**, 2410 (1986).
18) H. F. Tiersten, J. Appl. Phys. **40**, 770 (1969).
19) R. A. Waldron, IEEE Trans. Sonics Ultrason. **18**, 8 (1971).
20) H.-N. Lin, H. J. Maris, L. B. Freund, K. Y. Lee, H. Luhn, and D. P. Kern, J. Appl. Phys. **73**, 37 (1993).
21) G. A. Antonelli, H. J. Maris, S. G. Malhotra, and J. M. E. Harper, J. Appl. Phys. **91**, 3261 (2002).
22) V. N. Astratov, S. Yang, S. Lam, B. D. Jones, D. Sanvitto, D. M. Whittaker, A. M. Fox, M. S. Skolnick, A. Tahraoui, P. W. Fry, and M. Hopkinson, Appl. Phys. Lett. **91**, 071115 (2007).
23) S. Tamura, Phys. Rev. B **79**, 054302 (2009).
24) K. Yamazaki, T. Yamaguchi, and H. Yamaguchi, Jpn. J. Appl. Phys. **46**, L1225 (2007).
25) V. Damljanović and R. L. Weaver, J. Acoust. Soc. Am. **115**, 1572 (2004).
26) B. A. Auld, *Acoustic Fields and Waves in Solids* (Robert E. Krieger, Malabar, FL, 1990) 2nd ed., Vol. 1, p. 1.